

COORDINATION
COMPOUNDS

Crystal Structure of EuCeCuS₃

A. V. Ruseikina

Tyumen State University, ul. Semakova 10, Tyumen, 625003 Russia

e-mail: adeschina@mail.ru

Received November 10, 2015

Abstract—The crystal structure of EuCeCuS₃, a complex sulfide synthesized for the first time, has been solved using X-ray powder diffraction data. Crystals are rhombic, space group *Pnma*, Ba₂MnS₃ structural type, $a = 8.1023(1)$ Å, $b = 4.0386(1)$ Å, $c = 15.9022(2)$ Å, $V = 520.36(1)$ Å³, $Z = 4$, $\rho_{\text{calcd}} = 5.767$ g/cm³. The Eu, CeS₇ polyhedron incorporates the Eu and Ce atoms, which are randomly disordered over two crystallographic sites. The bond lengths $d_{\text{Eu,Ce-S}}$ range from 2.885 to 3.044 Å.

DOI: 10.1134/S0036023616110176

The crystal structures of ACeCuS₃ (A = Sr, Ba) were solved using X-ray powder diffraction data [1–3]. BaCeCuS₃ is isostructural to Eu₂CuS₃ [1, 2]. SrCeCuS₃ has two polymorphs of rhombic symmetry (space group *Pnma*): α -SrCeCuS₃ of BaLaCuS₃ structural type (at 970 K) with unit cell parameters $a = 11.1626(2)$ Å, $b = 4.0970(2)$ Å, and $c = 11.5307(1)$ Å and β -SrCeCuS₃ of Ba₂MnS₃ structural type (at 1170 K) with $a = 8.1393(3)$ Å, $b = 4.0587(2)$ Å, and $c = 15.9661(2)$ Å. The Sr and Ce atoms in α - and β -SrCeCuS₃ are observed to be disordered over two crystallographic sites. The site occupancy is 0.84:0.16 (α -) and 0.58:0.42 (β -), respectively [3]. The ratio between the radii of seven-coordinated ions $r_{\text{Ba}^{2+}} : r_{\text{Sr}^{2+}} : r_{\text{Eu}^{2+}} = 1.38 : 1.21 : 1.2$ [4] allows us to predict the formation of EuCeCuS₃. Close values of $r_{\text{Sr}^{2+}}$ and $r_{\text{Eu}^{2+}}$ enable EuCeCuS₃ to crystallize in one of the Ba₂MnS₃/BaLaCuS₃ structural types, and there is also some probability for the existence of polymorphs. No crystallographic data were found for EuCeCuS₃ in the literature.

Here, we report some results of solving the crystal structure of EuCeCuS₃ with the use of X-ray powder diffraction data.

EXPERIMENTAL

Cu₂S was synthesized from elementary copper (11–4 high purity grade) and sulfur (15–3 high purity grade) in ampoules. Ce₂S₃ and EuS were synthesized from oxides of TseO-L and EvO-Zh grade in an H₂S and CS₂ flow at 1300 K [5]. According to X-ray powder diffraction data, the synthesized sulfides were single phases and had a stoichiometric composition within chemical analysis error. EuCeCuS₃ was prepared by

alloying a mixture of initial sulfides EuS, Ce₂S₃, and Cu₂S at a ratio 2 : 1 : 1 in a graphite crucible placed into an evacuated and sealed quartz ampoule. The ampoule was heated in an electrical furnace to 1570 K and allowed to stand for 30 min. Cooling was performed in the switch-off furnace. Samples were annealed at 970 K for 4 months and at 1170 K for 2 months [6, 7].

X-ray powder diffraction analysis of EuCeCuS₃ was performed on a PANalytical X'Pert PRO diffractometer (CoK α radiation, graphite monochromator, PIXcel detector) within the angle range of $10^\circ \leq 2\theta \leq 140^\circ$. Samples were prepared by pounding with addition of octane in an agate mortar. The unit cell parameters were determined with the ITO software [8].

According to the data of X-ray powder diffraction and microstructural analysis (METAM LV-31 microscope), the 2EuS : 1Ce₂S₃ : 1Cu₂S sample annealed at 1170 K contained EuCeCuS₃ alone. Element distribution spectra were determined on a Philips SEM JEOL JSM-6510 LM scanning electron microscope at five different points on the surface of a sample. The compositions of all the analyzed areas corresponded to EuCeCuS₃. X-ray spectral microanalysis results coincided with theoretical values within a measurement accuracy of 0.2 wt %. The crystal structure of EuCeCuS₃ (annealing at 1170 K) was refined by the derivative difference minimization (DDM) method in the anisotropic approximation for all atoms with the reliability factors R-DDM = 4.88% and $R_F = 1.61\%$. The data for isostructural PbLaCuS₃ were used as an initial structural model [9]. Refinement was performed taking into account the effects of preferred orientation, anisotropic broadening of peaks, and sample surface roughness and displacement. Anion–cation distances and selected bond angles are given in Tables 1 and 2, respectively. The experimental, calculated, and differ-

Table 1. Interatomic distances (d) in the structure of β -EuCeCuS₃

Bond	$d, \text{\AA}$	Bond	$d, \text{\AA}$	Bond	$d, \text{\AA}$
(Ce1,Eu2)–S1	$2 \times 2.923(3)$	(Eu1,Ce2)–S1	3.014(4)	Cu–S1	$2 \times 2.354(2)$
(Ce1,Eu2)–S1	3.044(4)	(Eu1,Ce2)–S2	$2 \times 2.925(3)$	Cu–S2	2.365(5)
(Ce1,Eu2)–S2	2.969(5)	(Eu1,Ce2)–S2	$2 \times 2.984(3)$	Cu–S3	2.356(5)
(Ce1,Eu2)–S3	$2 \times 2.885(3)$	(Eu1,Ce2)–S3	$2 \times 3.058(4)$	$\langle \text{Cu–S} \rangle$	2.357(2)
(Ce1,Eu2)–S3	3.052(5)	$\langle (\text{Eu1,Ce2–S}) \rangle$	2.992(2)		
$\langle (\text{Ce1,Eu2)–S} \rangle$	2.954(2)				

ence X-ray powder diffraction patterns after DDM refinement are shown in comparison in Fig. 1. The crystal structures were visualized using the Diamond 3 software suite [10].

The $2\text{EuS} : 1\text{Ce}_2\text{S}_3 : \text{Cu}_2\text{S}$ sample annealed at 970 K contained two EuCeCuS_3 polymorphs, namely, 73.8% of Ba_2MnS_3 structural type ($a = 8.0991(1) \text{\AA}$, $b = 4.03978(4) \text{\AA}$, $c = 15.8979(1) \text{\AA}$) and 20.1% of BaLaCuS_3 structural type ($a = 11.1174(2) \text{\AA}$, $b = 4.07142(9) \text{\AA}$, $c = 11.4837(2) \text{\AA}$), which were denoted as β - and α -modifications, respectively, alongside with some admixtures, such as 0.6% of EuS , 0.9% of CuCeS_2 , and 4.6% of Eu_2CuS_3 . Since the sample represented a mixed phase and was poorly crystallized, no refinement was performed for the structure of EuCeCuS_3 (coordinates, thermal parameters, atomic site

occupancies). Longer annealing is required for the synthesis of a homogeneous α - EuCeCuS_3 sample.

RESULTS AND DISCUSSION

The X-ray powder diffraction pattern of β - EuCeCuS_3 (annealing at 1170 K) was indexed in terms of orthorhombic crystal system, Ba_2MnS_3 structural type, with unit cell parameters $a = 8.1023(1) \text{\AA}$, $b = 4.0386(1) \text{\AA}$, $c = 15.9022(2) \text{\AA}$; $V = 520.36(1) \text{\AA}^3$, $Z = 4$, and $\rho_{\text{calcd}} = 5.767 \text{ g/cm}^3$. β - EuCeCuS_3 has a layered-block structure (Fig. 2). Continuous chains of distorted CuS_4 tetrahedra sharing apical S1 atoms along direction [010] are spaced by seven-coordinated Sr and Ce atoms, which form one-capped trigonal $(\text{Eu,Ce})\text{S}_7$ prisms. The crystallographic sites of europium and cerium are mixed by 35%. Similar disorder-

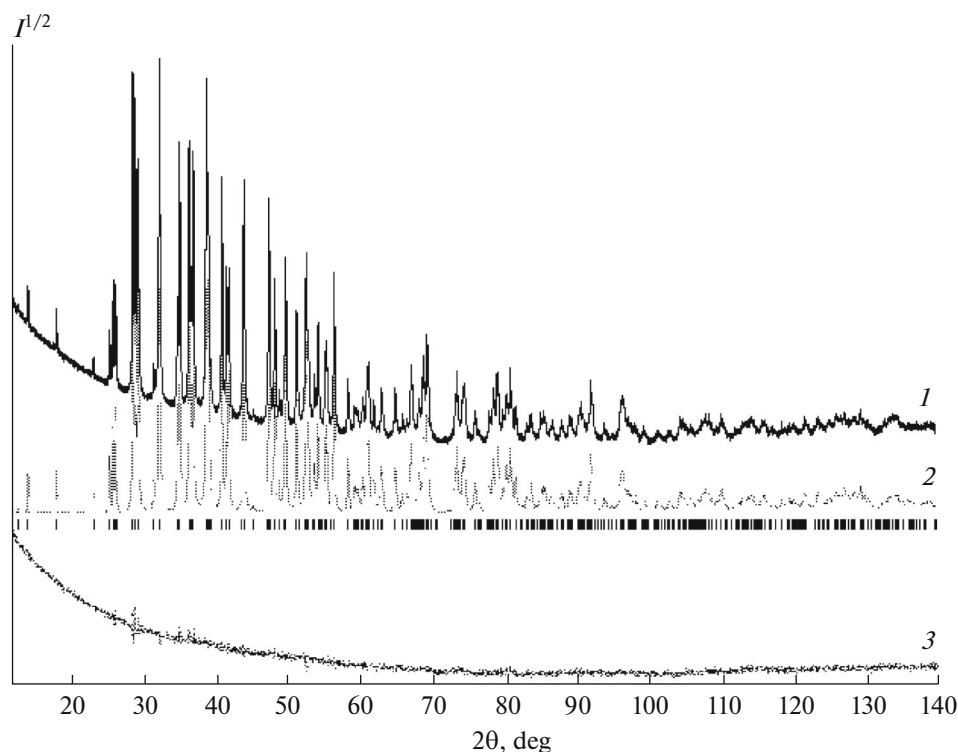


Fig. 1. (1) Experimental, (2) calculated, and (3) difference X-ray powder diffraction patterns of the $2\text{EuS} : 1\text{Ce}_2\text{S}_3 : 1\text{Cu}_2\text{S}$ sample after DDM refinement of its structure. Main phase peak positions are shown with strokes.

Table 2. Selected bond angles in the structure of β -EuCeCuS₃

Angle	ω , deg	Angle	ω , deg	Angle	ω , deg
S1(Ce1,Eu2)S1	87.40(9)	S1(Eu1,Ce2)S3	138.35(10)	S1CuS1	118.12(13)
S1(Ce1,Eu2)S1	78.00(8)	S2(Eu1,Ce2)S1	79.63(9)	S1CuS3	108.64(13)
S1(Ce1,Eu2)S2	78.47(9)	S2(Eu1,Ce2)S1	77.71(9)	S1CuS2	108.96(13)
S1(Ce1,Eu2)S3	125.12(10)	S2(Eu1,Ce2)S2	157.30(10)	S3CuS2	102.36(14)
S1(Ce1,Eu2)S3	143.98(10)	S2(Eu1,Ce2)S2	87.34(10)		
S2(Ce1,Eu2)S1	147.24(10)	S2(Eu1,Ce2)S2	89.3(10)		
S2(Ce1,Eu2)S3	68.78(10)	S2(Eu1,Ce2)S2	85.18(10)		
S3(Ce1,Eu2)S1	80.34(9)	S2(Eu1,Ce2)S3	131.86(10)		
S3(Ce1,Eu2)S1	158.33(10)	S2(Eu1,Ce2)S3	75.84(98)		
S3(Ce1,Eu2)S1	87.84(10)	S2(Eu1,Ce2)S3	121.82(10)		
S3(Ce1,Eu2)S2	121.12(10)	S2(Eu1,Ce2)S3	68.50(10)		
S3(Ce1,Eu2)S3	74.19(10)	S3(Eu1,Ce2)S3	82.65(10)		
S3(Ce1,Eu2)S3	88.83(10)				

ing also appears in isostructural $ALnCuS_3$ crystals ($A = \text{Eu, Sr, Pb}$; $Ln = \text{La, Ce, Pr}$) [3, 5, 9, 11, 12].

A one-capped trigonal $Ce1S_7$ prism is built of $2S1 + S1 + S2 + 2S3 + S3$ atoms with an average $Ce1-S$ distance of 2.954 Å (Table 1) at a theoretical value of 2.955 Å calculated from the ionic radii $r_{Ce^{3+}} = 1.07$ and $r_{Eu^{2+}} = 1.20$ Å ($CN = 7$) [4] with consideration for the site occupancy $Ce1 : Eu2 = 0.652 : 0.348$. One-capped trigonal $Ce1S_7$ prisms share $2 \times S1S1$ and $2 \times S3S3$ edges along axis a and $2 \times S3S1$ edges along axis b to form two-dimensional networks in plane ab . A one-capped trigonal $Eu1S_7$ prism is built of $S1 + 2S2 + 2S2 + 2S3$ atoms with an average $Eu1-S$ distance of 2.992 Å (theoretical value, 2.994 Å). $Eu1S_7$ prisms share $2 \times S2S2$ edges along axis a and $2 \times S2S2S3$ faces along axis b to form two-dimensional networks in plane ab . One-capped trigonal $Eu1S_7$ and $Ce1S_7$ prisms share edges to form a three-dimensional network with channels accommodating Cu^{2+} ions.

The structural characteristics of β -EuCeCuS₃ are intermediate between $EuLaCuS_3$ [11] and β -EuPrCuS₃ [12]. The unit cell parameters of $EuLnCuS_3$ ($Ln = \text{La}$ [11], Ce, Pr [12]) annealed at 1170 K naturally decrease:

$$a = 8.1366 (\text{EuLaCuS}_3 [11]) \rightarrow 8.1023 (\beta\text{-EuCeCuS}_3) \rightarrow 8.0786 (\beta\text{-EuPrCuS}_3 [12]) \text{ \AA};$$

$$b = 4.0586 (\text{EuLaCuS}_3 [11]) \rightarrow 4.0386 (\beta\text{-EuCeCuS}_3) \rightarrow 4.0288 (\beta\text{-EuPrCuS}_3 [12]) \text{ \AA};$$

$$c = 15.9822 (\text{EuLaCuS}_3 [11]) \rightarrow 15.9022 (\beta\text{-EuCeCuS}_3) \rightarrow 15.8389 (\beta\text{-EuPrCuS}_3 [12]) \text{ \AA}.$$

The average values of d_{Ln-S} and d_{Cu-S} are also observed to sustain a natural decrease with descending $r_{Ln^{3+}}$ in the series of $EuLnCuS_3$:

$$d_{Ln-S}: 2.975 (d_{La1-S} [11]) \rightarrow 2.954 (d_{Ce1-S}, \text{Table 1}) \rightarrow 2.719 (d_{Pr1-S} [12]) \text{ \AA};$$

$$3.003 (d_{La2-S} [11]) \rightarrow 2.992 (d_{Ce2-S}, \text{Table 1}) \rightarrow 2.983 (d_{Pr1-S} [12]) \text{ \AA};$$

$$d_{Cu-S}: 2.359 [11] \rightarrow 2.357 (\text{Table 1}) \rightarrow 2.348 [12] \text{ \AA}.$$

Hence, the established X-ray and structural parameters of β -EuCeCuS₃ agree with a natural change in the parameters, bond lengths, and structural types obtained for the series of $EuLnCuS_3$ ($Ln = \text{La, Pr, Nd, Sm-Dy, Tm-Lu}$) correlated with a change in the Ln^{3+} ionic radius in the earlier works [5–7, 11–13].

The crystal structures of $ACeCuS_3$ ($A = \text{Sr, Eu}$) are observed to have some similarity due to close $r_{Sr^{2+}}$ and $r_{Eu^{2+}}$. The various bond lengths $d_{(A,Ce)-S}$ in $ACeCuS_3$ ($A = \text{Sr, Eu}$) produce a difference between their unit cell parameters and volumes and X-ray densities. Small values of the average bond lengths $d_{Eu1-S} = 2.992(2)$ Å and $d_{Ce1-S} = 2.954(2)$ Å ($EuCeCuS_3$) in comparison with $d_{Sr1-S} = 3.004(2)$ Å and $d_{Ce1-S} = 2.971(2)$ Å ($SrCeCuS_3$ [3]) are due to the facts that

(1) The covalent component of the $(\text{Eu,Ce})-S$ bond is less pronounced than for the $(\text{Sr,Ce})-S$ bond. This agrees with the theoretical notions about that rare-earth elements (as transition metals) have an insufficient bond ionicity in comparison with alkali-earth elements [14]; and

(2) $r_{Eu^{2+}} < r_{Sr^{2+}}$. This in turn is caused by the electron structure of Sr ($5s^2$) and Eu ($4f^7 5d^0 6s^2$) and the lanthanide contraction effect.

It is likely that small differences between $r_{A^{2+}}$ and $r_{Ce^{3+}}$ ($\Delta r_{Sr-Ce} = 11.5\%$, $\Delta r_{Eu-Ce} = 10.8\%$) cause the displacement of A^{2+} and Ce^{3+} crystallographic sites.

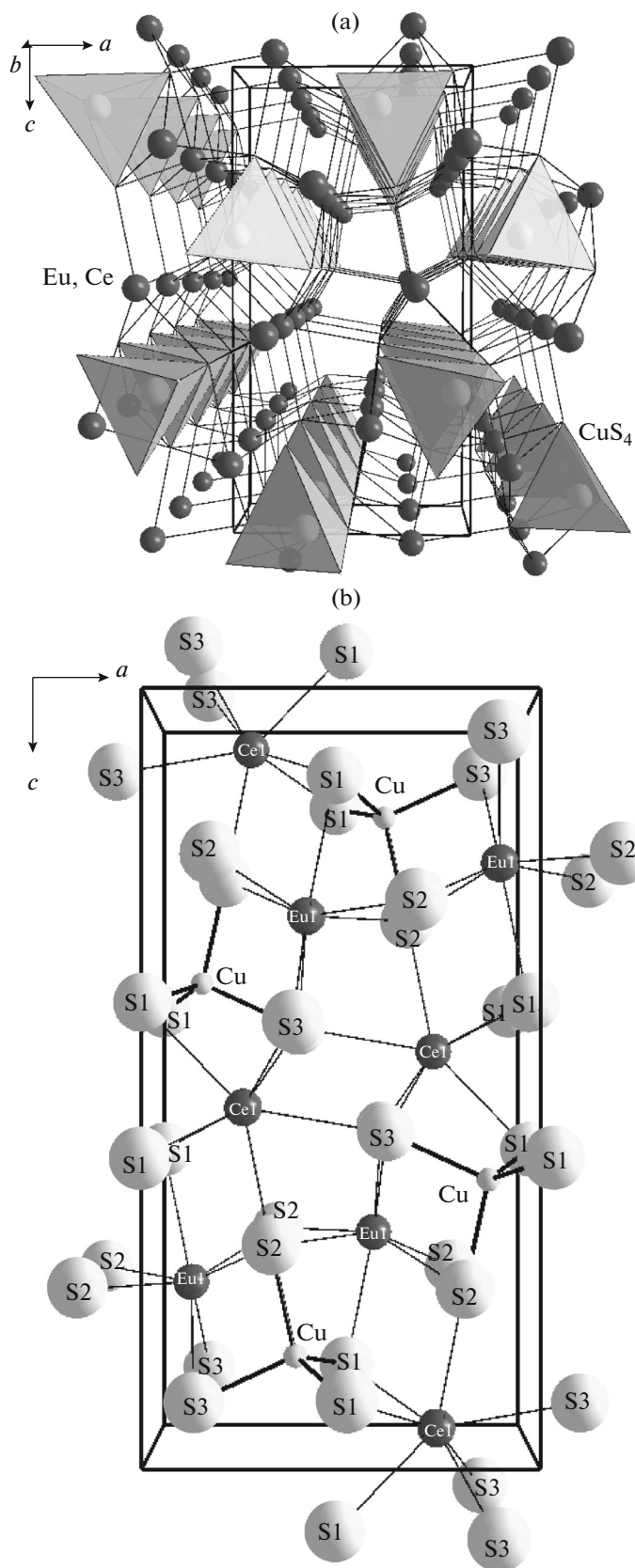


Fig. 2. Projections [010] for the structure of β -EuCeCuS₃.

Hence, two polymorphs have been revealed for EuCeCuS₃: low-temperature α -EuCeCuS₃ (BaLaCuS₃ structural type) and high-temperature β -EuCeCuS₃ (Ba₂MnS₃ structural type), which are similar to the modifications appearing for EuPrCuS₃ [12] and SrCeCuS₃ [3]. The crystal structure of β -EuCeCuS₃ (annealing at 1170 K) has been solved. The cerium and europium atoms in this structure are randomly disordered over two crystallographic sites. It should be expected that the disordering of rare-earth element atoms over sites will be retained at a lower annealing temperature (970 K) as for SrCeCuS₃ [3]. Longer annealing is required for the synthesis of a homogeneous α -EuCeCuS₃ sample (annealing at 970 K).

ACKNOWLEDGMENTS

The author of this paper is grateful to L.A. Solov'ev, a researcher of the Institute of Chemistry and Chemical Technology of the Siberian Branch of the Russian Academy of Sciences (Krasnoyarsk), for performing the X-ray powder diffraction analysis of sulfide.

This work was financially supported by state task no. 2014/228, research project no. 996.

REFERENCES

1. P. Wu, A. E. Christuk, and J. A. Ibers, *J. Solid State Chem.* **110**, 337 (1994).
2. L. A. Koscielski, *Z. Anorg. Allg. Chem.* **638**, 2585 (2012).
3. A. V. Ruseikina, L. A. Solov'ev, *Russ. J. Inorg. Chem.* **61**, 482 (2016).
4. R. D. Shannon, *Acta Crystallogr., Sect. A* **32**, 751 (1976).
5. A. V. Ruseikina, L. A. Solov'ev, and O. V. Andreev, *Russ. J. Inorg. Chem.* **59**, 196 (2014).
6. A. V. Ruseikina, L. A. Solov'ev, O. V. Andreev, and A. A. Kislitsyn, *Russ. J. Inorg. Chem.* **59**, 1109 (2014).
7. A. V. Ruseikina, L. A. Solov'ev, M. S. Molokeev, and O. V. Andreev, *Russ. J. Inorg. Chem.* **57**, 79 (2012).
8. J. W. Visser, *J. Appl. Crystallogr.* **2**, 89 (1969).
9. T. D. Brennan and J. A. Ibers, *J. Solid State Chem.* **97**, 377 (1992).
10. K. Brandenburg, DIAMOND: Visual Crystal Structure Information System CRUSTAL IMPACT (Postfach 1251, D-53002 Boon).
11. A. V. Ruseikina, L. A. Solov'ev, and O. V. Andreev, *Russ. J. Inorg. Chem.* **57**, 574 (2012).
12. A. V. Ruseikina, L. A. Solov'ev, and O. V. Andreev, *Russ. J. Inorg. Chem.* **58**, 1231 (2013).
13. M. Wakeshima, F. Furuuchi, and Y. Hinatsu, *J. Phys.: Condens. Matter* **16**, 5503 (2004).
14. D. V. Shriver and P. W. Atkins, *Inorganic Chemistry*, 3rd ed. (Freeman, New York, 1999; Mir, Moscow, 2004).

Translated by E. Glushachenkova